2021 IEEE/RSJ International Conference on Intelligent Robots and Systems (IROS)
September 27 - October 1, 2021. Prague, Czech Republic

Parallel Variable Stiffness Actuators

Chase W. Mathews and David J. Braun

***Abstract*— In this paper, we introduce a new type of compliant actuator named the Parallel Variable Stiffness Actuator (PVSA) which consists of a variable stiffness spring placed in parallel with a direct-drive motor. Parallel variable stiffness actuators provide (i) high-fidelity force control and (ii) controllable energy storage, as they inherit the benefits of direct-drive motors and variable stiffness springs. We present a compact design of the PVSA using a flat motor connected to an adjustable mechanical advantage torsional spring. We show that this PVSA is (1) not subject to the fundamental force control bandwidth limitation of series elastic and variable stiffness actuators, and most notably, (2) enables resonant energy accumulation despite the limited deformation of the spring and the constrained motion of the load attached to the actuator. The latter differentiates parallel variable stiffness actuators from fixed-stiffness parallel elastic actuators. PVSAs may be used with smaller direct-drive motors to match the peak power of larger motors without compromising force control fidelity. PVSAs may be used to implement resonant forcing under joint angle limitations in walking, jumping, running, swimming robots, or robotic exoskeletons used to augmented human motion in the aforementioned tasks.**

I. Introduction

Compliant actuators have demonstrated potential in the areas of industrial robot safety, rehabilitation devices, and mobile robots [1]. One of the most common compliant actuators is the Series Elastic Actuator (SEA); in its most basic arrangement, the SEA is the addition of an elastic element (e.g. a spring) between the load and the primary actuator (e.g. a motor) [2]. The passive compliance of the spring functions to protect the primary actuator (typically highly geared) from shock loads, allow safe force control of the load, and store elastic potential energy [3]. SEAs can be found in devices such as as ankle prostheses [4], knee prostheses [5], and powered arm exoskeletons [6]. One modification the SEA is the Variable Stiffness Actuator (VSA), in which a Variable Stiffness Spring (VSS) is used in place of a fixed-stiffness spring [7]. The variable passive compliance allows for control of frequency response and actuation speed, and has been used in ankle exoskeletons [8], [9] and robotic joints [10]. However, series compliant actuators have a few pitfalls that limit their practicality in human augmentation and robotic devices: (i) it is energetically expensive to generate force without motion, (ii) all force generated by the motor must first pass through the spring, which limits the force control bandwidth of the actuator.

Chase W. Mathews and D. J. Braun are with the Advanced Robotics and Control Laboratory within the Center for Rehabilitation Engineering and Assistive Technology, Department of Mechanical Engineering, Vanderbilt University, Nashville, Tennessee 37235, USA.
E-mail: chase.w.mathews@vanderbilt.edu
E-mail: david.braun@vanderbilt.edu

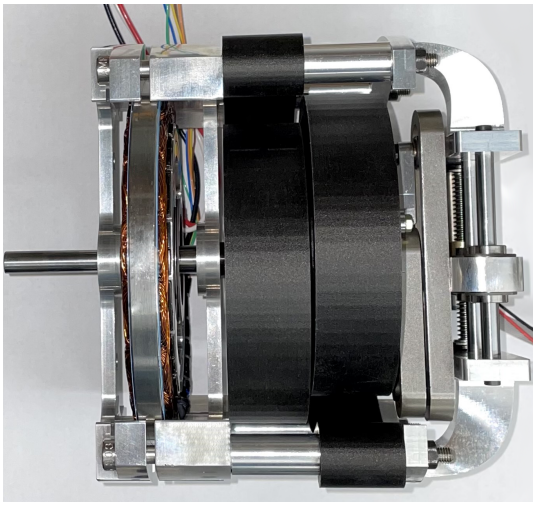

Fig. 1. Prototype parallel variable stiffness actuator.

Because of these limitations, SEAs and VSAs are not well suited for high-energy tasks.

For most actuators, there is a trade-off between torque density and compliance. Gears are typically used to increase the torque density of electric motors, but come with the cost of lower efficiency, reduced precision, and slower response times [2]. Thus, it is desirable to minimize the gearing when possible. Recent developments of torque-tense motors have enabled the use of low gearing or even direct drive robotic joints. For example, the MIT Cheetah [11] is a quadruped robot which runs using highly backdrivable motors. Direct-drive motors still have much lower torque density than comparable gearmotors. One way to amplify output torque of a motor without compromising efficiency or compliance is to use a mechanical spring in parallel with the motor, i.e. a Parallel Elastic Actuator (PEA). PEAs have demonstrated lower energy consumption and peak power requirements as compared to SEAs [12]–[15] Parallel elasticity especially shows promise in assistive devices since the elastic elements can offload force from the muscles; for example, a walking exoskeleton [16] and a jogging exoskeleton [17], [18] utilized parallel elastic elements to reduce metabolic energy cost. One limitation for PEAs is the use of fixed stiffness springs; fixed stiffness springs only promote efficient cyclic motion at one resonant frequency and it is energetically expensive to oscillate at different frequencies.

In this paper, we introduce a new class of Parallel Variable Stiffness Actuators (PVSAs) which consist of a direct-drive motor arranged in parallel with a variable stiffness spring (Figure 1). The PVSA provides high fidelity force control

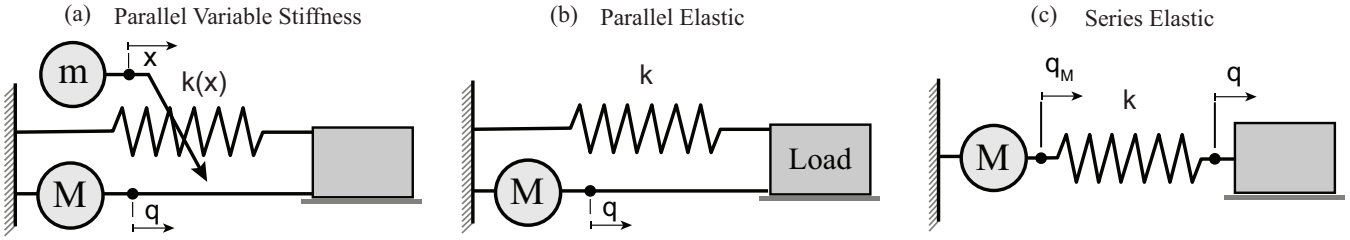

Fig. 2. Compliant actuators driven by a large motor (M) that generates force and supplies energy and one small motor (m) that modulates the stiffness of the spring in parallel variable stiffness actuators; q denotes the position of the load, x is the position of the small motor while q_M is the position of the motor in series elastic actuators.

and controllable energy storage with inherent compliance. For cyclic motions, the PVSA has the ability to amplify the mechanical power of the direct-drive-motor by using the spring as a mechanical energy storage reservoir. The VSS has the unique ability to modulate the resonant frequency of the system; this expands the power amplification space to include frequency modulation, instead of the more typical amplitude modulation to accumulate energy. Frequency modulation allows for kinetic energy accumulation under motion constraints, such as in jumping , which is important for robots and devices subject to joint angle limitations [19].

We present a compact design of a PVSA which has high motor power to weight ratio, high energy storage to weight ratio, and large range of stiffness change. Our design features a modular architecture where the variable stiffness mechanism is connected to a motor similar to how a gearbox is connected to a motor, and where springs with different energy storage capacity and stiffness can be interchanged similar to gearboxes with different gear ratios.

II. Parallel Variable Stiffness Actuators

The PVSA consists of two main components placed in parallel: a variable stiffness spring (VSS) and a direct drive motor (DDM). A conceptual model of a PVSA is shown in Fig. 2a together with two alternative actuators: the parallel elastic actuator (PEA) Fig. 2b, and the series elastic actuator (SEA) Fig. 2c.

A. Mathematical Model

In this section, we present one of the simplest models of PVSAs. The model consists of (1) a larger direct drive motor (M) – pure force generator – that acts on the load, (2) a variable stiffness spring that acts on the load, and (3) the stiffness modulating mechanism driven by a small motor (m). The equations that govern the dynamics of the load and the stiffness modulating mechanism are given by:

$$M\ddot{q} + k(x)q = F \tag{1}$$

$$m\ddot{x} + \frac{1}{2}\frac{dk(x)}{dx}q^2 = F_m \tag{2}$$

where M is the mass of the load, q is the position of the load, k is the spring stiffness, x is the position of the stiffness modulating motor, F is the external force acting on the load, m is the mass of the stiffness modulating mechanism while F_m is the motor force.

The relation between the stiffness of the actuator k and the position of the motor x that modulates the stiffness of the spring, depends on the stiffness modulating mechanism [20]. For example, the following relations

$$k(x) = c_0 + c_1 x, \quad k(x) = \frac{c_0}{x}, \quad k(x) = \frac{c_0}{x^3} \tag{3}$$

define the stiffness of an antagonistic stiffness modulator [21], [22] where x is the extension of the spring, a helical spring [23], torsional leaf-spring [24] or a bending leaf-spring [25] where x is the length of the spring.

B. Force Control and Resonant Forcing

In this section, we demonstrate the main benefits of PVSAs which are (i) high fidelity force control compared to SEAs and (ii) resonant forcing under motion constraint when compared to PEAs.

(i) *High fidelity force control:* In PVSAs, the force of the driving motor F is directly applied to the load, similar to direct-drive actuators. Consequently, assuming an ideal feedback loop, the force control bandwidth is infinite. In practice, finite sampling times limit the force control bandwidth of PVSAs (Fig. 2a) the very same way as they limit the force control bandwidth of direct-drive actuators. However, the bandwidth is only dependent on the time constant of the motor current dynamics while it is independent of the time constant of the motor position dynamics. The same does not apply to series elastic actuators (Fig. 2c) or the more general class of variable stiffness actuators [11] (not shown in Fig. 2), as in both of these actuators, the motor force cannot be directly applied to the load; it can only be applied through the spring. As a result, the force control bandwidth in series elastic and variable stiffness actuators is determined by the time constant of the motor position dynamics which may be three orders of magnitude larger (fraction of a second) than the time constant of the motor current dynamics (fraction of a millisecond). The difference between the force control bandwidth of a PVSA compared to a SEA (or VSA) can be best exemplified by a task that requires resonant forcing.

(ii) *Resonant forcing:* Let us assume that we aim to generate oscillatory motion of a robot limb, similar to the oscillatory motion of the hip in human running or swimming. In this task, we may assume that the oscillations start with low frequency, corresponding to jogging or casual swimming, while they end at a high frequency, as in sprinting. Also, we

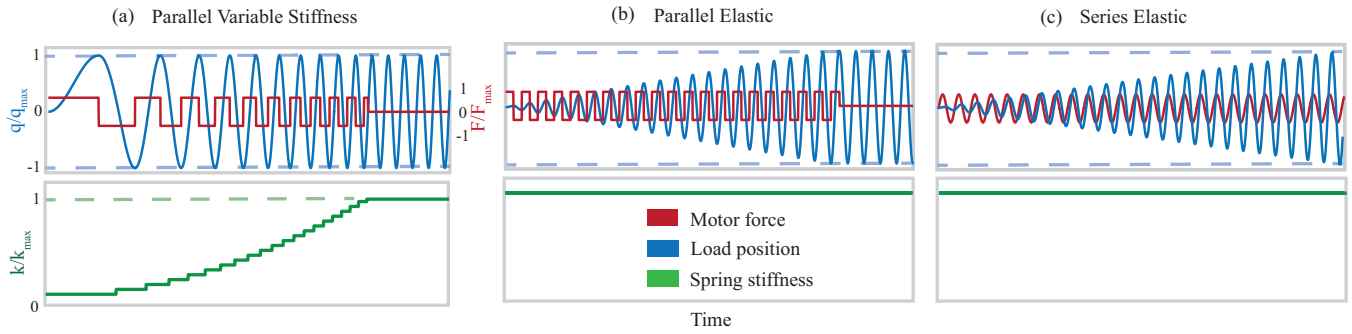

Fig. 3. Resonant forcing of a linear oscillator using (a) a parallel variable stiffness actuator, (b) a parallel elastic actuator, and (c) a series elastic actuator. The actuators are assumed to have instantaneous force generation and stiffness modulation. In the case of the SEA, the force generation is filtered through general closed-loop positioning dynamics of the motor.

aim to achieve this task using a weak, force limited actuator, similar to a force limited muscle, and we aim to ensure that the amplitude of the oscillatory motion does not exceed a set constraint which may be interpreted as a motion range or joint angle limitation in robots or humans.

Resonant forcing is a useful method of actuation using a fast but weak actuator. These are the main characteristics of a typical direct-drive motor. Here we assume that bandwidth of the ideal motor is infinite while the motor can only produce limited force:

$$F \in [-F_{\max}, F_{\max}]. \tag{4}$$

Resonant forcing also requires a spring with sufficient energy storage capacity. The energy storage capacity of a typical linear spring is defined by its stiffness and the maximum allowable deflection of the spring $E \leq E_{\max} = \frac{1}{2} k q_{\max}^2$. Here we assume that the stiffness of the spring can be changed in a finite range and that the deflection of the spring is limited

$$k \in [k_{\min}, k_{\max}] \quad \text{and} \quad q \in [-q_{\max}, q_{\max}]. \tag{5}$$

In resonant forcing, the motor force $F = \pm F_{\max}$ is applied as a constant, where the direction of the force changes at every peak of the load position q (see Fig. 2a). In this way, the amplitude will grow without bound (assuming no energy dissipation), thereby, the constraints on the load position $q(t) \in [-q_{\max}, q_{\max}]$ may not be maintained at all times t. However, we may limit the amplitude of the oscillator to ensure the second condition in (5), or even maintain the amplitude of the oscillator at every cycle

$$\max_t q(t) = q_{\max} \quad \text{and} \quad \min_t q(t) = -q_{\max}, \tag{6}$$

by changing the stiffness of the spring when it does not store energy $q \approx 0$. The energy balance of the system shows the relation between the stiffness k_n, external force F_n, and the maximum amplitude of oscillations q_{max}:

$$E_{n+1} = E_n + F_n q_{max} \Rightarrow \frac{1}{2} k_{n+1} q_{max}^2 = \frac{1}{2} k_n q_{max}^2 + F_n q_{max} \tag{7}$$

From (7), a relationship between amplitude, resonant forcing, and stiffness is established:

$$k_{n+1} = k_n + \frac{2F_n}{q_{\max}}. \tag{8}$$

where n and $n+1$ denote the current and the next half oscillatory cycles. Assuming $k_0 = k_{\min}$ and $k_n < k_{n+1}$, the frequency of the oscillations will increase according to the following relation:

$$f_n = \frac{1}{\pi\sqrt{m}} \left(\frac{1}{\sqrt{k_n}} + \frac{1}{\sqrt{k_n + \frac{2F_n}{q_{\max}}}} \right)^{-1} \tag{9}$$

Therefore, by changing the stiffness of the spring $k_{\min} \leq k_0 < k_1 < \ldots < k_n < \ldots < k_N \leq k_{\max}$, we may reach a desired frequency f_d in finitely many oscillations N, and maintain the desired frequency using zero force and the optimal stiffness:

$$f_d = f_N, \quad F_N = 0, \quad k_N = \frac{4}{\pi^2 m} \frac{1}{f_d} \leq k_{\max}. \tag{10}$$

Increasing the frequency of the oscillations while the amplitude is maintained constant (6) leads to energy accumulation $E_{\min} \leq E_0 < E_1 < \ldots < E_n < \ldots < E_N \leq E_{\max}$. Maintaining the constant amplitude condition (6) is possible if the minimum amount of energy exceeds a lower limit $E_0 \geq \frac{1}{2} k_{\min} q_{\max}^2$ while the maximum amount of energy does not exceed the energy capacity of the spring $E_N \leq \frac{1}{2} k_{\max} q_{\max}^2$.

In this section we have demonstrated the principle of constant amplitude resonant forcing achievable by a PVSA by assuming the simplest linear spring and no energy dissipation. The same principle extends to weakly dissipative nonlinear oscillators [26], and may be useful to accumulate energy – increase the frequency of an oscillatory limb motion subject to joint angle limitation – in robots driven by small motors.

C. Comparison to Other Compliant Actuators

In order to compare PVSAs to PEAs and SEAs, we assume that all three have the same energy storage capacity, and that the maximum motor force is also the same in all these actuators shown in Figs. 2 and 3.

Compared to PVSA (Fig. 3a), the ability of a SEA to accumulate energy is tied to the closed loop position control bandwidth of the motor. SEAs typically use highly geared motor drives with position control in order to create a position differential between the load and the motor. The maximum work done by SEA depends on its position control

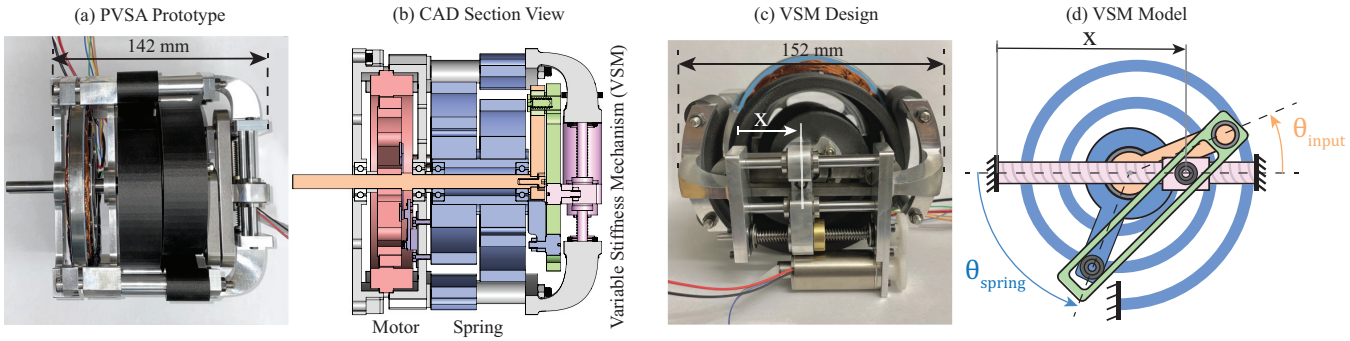

Fig. 4. (a) Top down view of the PVSA prototype. (b) Cross-sectional CAD view of the PVSA prototype. (c) Back view of the constructed prototype. (d) Model of the variable stiffness mechanism (VSM).

bandwidth which may be three orders of magnitude lower than the force control bandwidth of the motor. Because of this, the SEA take more cycles than the PVSA to accumulate the same amount of energy (Fig. 3c).

Compared to the PVSA (Fig. 3a), the PEA can do less work in every cycle, and thereby, needs more cycles to accumulate the same amount of energy (Fig. 3b). The maximum work done by PEA is $F_{\max} q_{\max,n} \leq F_{\max} q_{\max}$ where the amplitude can only gradually increase according to

$$q_{\max,n+1} = q_{\max,n} + \frac{F_{\max}}{k_{\max}} \leq q_{\max}.$$

Because of this, the PEA takes more cycles than the PVSA to accumulate the same amount of energy (Fig. 3a,b).

The higher number of cycles could be detrimental for tasks with collision and hysteretic energy losses. Depending on the system natural frequency, the ability of the motor to apply force may be attenuated as well since the system is always operating at the spring resonant frequency. In some tasks, the limitation on the range of motion by stiff springs may cause instability problems; for example, a higher stiffness ankle exoskeleton as developed in [16] actually increased metabolic cost, likely due to an interference with muscle coordination. Researchers have mitigated these problems in parallel elasticity to some extent by using a nonlinear dual-stage spring [14]; however, the spring resonance must be optimized for a specific task. The PVSA would work best for tasks that (i) need full range of motion while accumulating energy and (ii) are subject to disturbances and variance.

III. Design of the PVSA

In this section, we present a prototype PVSA (Fig. 4a). The prototype is composed of the variable stiffness spring mechanism, a custom made fiberglass spring, and a direct drive motor (Fig. 4b). The prototype was designed based on the following four objectives:

1) Maximize energy storage capacity of the actuator.
2) Minimize energy losses of the actuator.
3) Maximize volumetric efficiency; similar to a gearbox.
4) Make a modular design, such that the spring can easily be interchanged to fit system requirements.

A. Variable Stiffness Spring Mechanism

The variable stiffness mechanism (Fig. 4c,d) is based on an adjustable mechanical advantage design such as the AwAS [27], AwAS-II [28], HDAU [29], and vsaUT-II [30]. We have chosen the variable pivot point design to keep the energy storage of the device independent of the stiffness. This is not true for VSS mechanisms where the effective length of the spring is changed to modulate stiffness [31]. If the pivot point drive train passively locks, then the VSS is able to maintain a certain stiffness passively. This is why an antagonistic VSS setup was also not chosen, as it requires increasing energy to maintain a given stiffness [7], [32].

Assuming small-angle deflections, the stiffness of the variable pivot point spring (Fig. 4d) can be represented with the following equation:

$$k(x) = k_{\text{spring}} \left(\frac{x}{l-x}\right)^2 \tag{11}$$

where k_{spring} is the stiffness of the spring, x is the position along the lever arm, and l is the length of the lever arm. According to this equation a large range of stiffness is achievable; theoretically the range of achievable stiffness is $[0, \infty]$ (if the pivot point is placed at the ends of the lever arm).

The equation of motion for the small stiffness modulating motor (2) is the following:

$$m\ddot{x} = -k_{\text{spring}} l \frac{x}{(l-x)^3} q^2 + F_m \tag{12}$$

This equation shows that when the deflection of the spring is zero (when the spring does not store energy) a small motor can change the stiffness of the spring without working against the spring. If the device is self locking, such as with a lead-screw, the force required to maintain position by the motor F_m is zero. Because of these two features, a small and lightweight motor can be used to drive the VSS mechanism. Because the modulation motor must be operated at a small range around zero deflection, $\pm\theta_{inc}$, the modulation drive must be fast enough to increment position within this range. Given a maximum load frequency ω_{max} and amplitude A, the desired positioning time Δt (the time it takes to increment stiffness k_n to k_{n+1}) must satisfy $\Delta t < 2\theta_{inc}/(A\omega_{max})$.

To convert the lever arm mechanism from a linear displacement mechanism to an angular displacement mechanism, two linkages were added at each end to relate input angle to the spring deflection angle as depicted in Fig. 4d. Since the link at each end of the lever arm both connect back to the same axis of rotation, the center of a torsion spring can be mounted about an arbor on the main shaft. This arrangement also allows the linkages to fit into a cylindrical footprint.

A lead screw drive was chosen as the pivot positioning actuator since it is self-locking. A direct driven Maxon DCX-22L motor was used for the lead screw modulator. The range of mechanical advantage adjustment of this spring was found through a geometric analysis of the linkages. In the specific mechanism design as shown in Fig. 4d, the range of mechanical advantage achieved was $[0.39, 2.8]$.

B. Spring Design

Because the variable stiffness mechanism uses an adjustable mechanical-advantage design, any torsion spring form factor would work. The main design goals of the spring are to (1) maximize energy storage per volume, (2) demonstrate low hysteresis, and (3) be easily manufactured. We selected a spiral torsion spring, these springs demonstrate large volumetric energy storage densities as a long length of spring can be coiled in a compact manner. The base torsional stiffness k_{spring} can be modeled as the following [33], [34]:

$$k_{\text{spring}} = \frac{Ebh^3}{12L} \tag{13}$$

where E is Young's modulus, b is the spring width, h is the spring thickness, L is the effective length of the spring.

The spring will operate in the elastic regime for small deflections. If the spirals are spaced far enough at this deflection, the spring also avoids colliding with itself which causes nonlinear stiffness effects and reduced efficiency. Flat spiral springs do not have the same properties in counterclockwise rotation as in clockwise rotation, one way to account for this is by de-clutching the springs during extension [35]. However, this results in a lower energy density since one spring is disengaged at all times. Another way is to mount two springs in opposite configurations such that one is in extension and one is in compression. In this setup, the stiffness will average out for both directions.

Another advantage of spiral torsion springs is the ease of manufacturing; the flat design is ideal for 3D printed, rolled, or cast materials. With the development of continuous fiber fabrication (CFF), strands of fiberglass can be laid along the length of the spiral spring. We use continuous fiberglass to fabricate the springs shown in Figure 4a,b. 3D printed continuous fibers demonstrate similar mechanical properties to 6061 Aluminum alloys with the design freedom of 3D printing.

C. Direct Drive Motor

The direct drive motor should be selected based on geometry and power requirements; generally, the torque capability of a motor is proportional to its diameter [36]. The function of the drive motor in the PVSA is twofold: (1) it must generate enough torque to overcome system damping and (2) it must apply torque to change stiffness $k_{n+1} - k_n \propto F_n$ according to (8). Therefore, the minimum motor torque in PVSA is defined by system damping, while the maximum motor torque defines the transient time required for the system to reach the desired oscillation frequency. Unlike in a direct drive actuator, the motor torque does not define the maximum torque of the parallel variable stiffness actuator .

We use an Allied Motion MF0127008 brushless frameless motor (Fig. 4a,b) which has a continuous torque rating of 1.6 Nm and a motor constant of 0.296 Nm/A. The housing both supports the stator of the motor and the springs. The springs and stiffness modulator mechanism were attached to the back of the motor shaft while the output of the actuator is at the front of the shaft. An AMS AS5304A offset-axis magnetic encoder and axial magnet were placed inside of the rotor for precise position measurements.

D. Overall Design

The mechanical design (Fig. 4) satisfies all of the initial design objectives by (1) using torsion spiral springs, (2) using a self-locking stiffness modulator, (3) having little unused space within the actuator volume, and (4) allowing easy swapping of the three components, motor, spring, and stiffness modulator depending on task.

IV. Evaluation

The analytical investigation presented in Section II was based on several simplifying assumptions, such as instantaneous force generation of the motor, instantaneous stiffness change, and zero damping. In this section we investigate the performance of our PVSA actuator using a simple experiment that is not subject to the aforementioned assumptions. In the experiment, a pendulum (0.4m long and 2kg) was attached to the PVSA, and the actuator was used to speed up the oscillation of the pendulum from its natural frequency of 0.9Hz to a desired frequency of 2Hz while maintaining an amplitude of $\pm$30deg. This experiment was used to emulate the speeding up of leg swing from walking and running.

A controller was implemented to switch the direction of the drive motor's torque based on the motion of the pendulum, such that the motor always applies torque in resonance with the motion of the pendulum. The stiffness modulator was set to increment stiffness within a range of $\pm$5deg and used a simple PD controller to regulate the position of the pivot point, see Fig. 4c,d.

The results are shown in Fig. 5 for the position, motor input, spring stiffness, PVSA torque, and electrical power consumption during a representative trial. The motor torque was calculated by multiplying the instantaneous drawn motor current by the torque constant. The PVSA torque was estimated by separating out the gravitational torque contribution of the pendulum $\tau_{\text{PVSA}} \approx ml^2\ddot{\theta} + mgl\sin\theta$, where m is the mass of the pendulum and l is the distance from the shaft to the center of the weight Fig. 5a. The electrical power

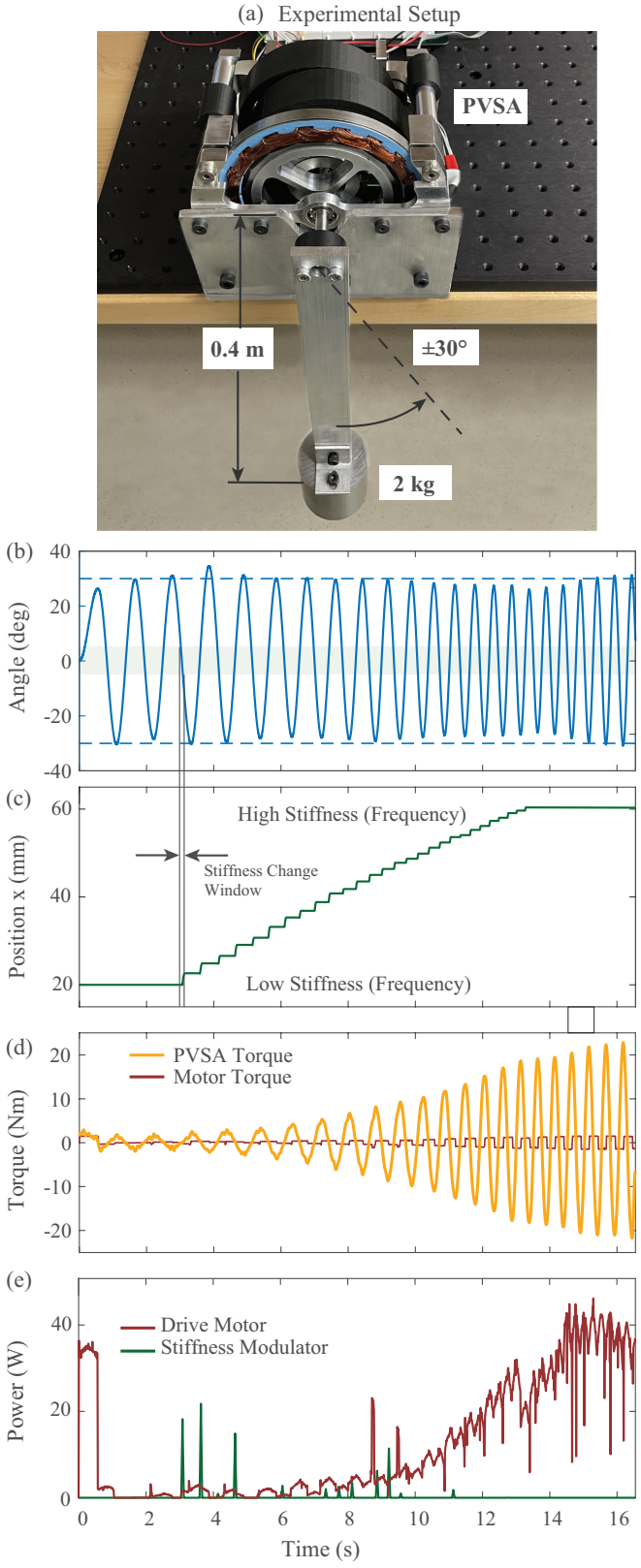

Fig. 5. (a) Experimental setup. (b) Pendulum angle q. (c) Position of the pivot point in the stiffness modulating subsystem x. (d) Actuator torque and the input drive motor torque. (e) Electrical power consumption of the drive motor and the stiffness modulating motor.

consumption was calculated by multiplying the consumed current by the motor voltage. Figure 5 shows that the PVSA is able to (i) accumulate energy within a set motion range limitation by increasing the frequency of the oscillations with negligible energy cost from the stiffness modulator (Fig. 5b,c,e-green), (ii) amplify the torque produced by the actuator 15 times within 16s (Fig. 5d), and (iii) maintain fast oscillations with a steady state power consumption of 37 W (Fig. 5b,e-red). This power is required to compensate for the hysteretic energy losses and motor inefficiency.

V. Conclusion

This work presented a parallel variable stiffness actuator, which has the ability to accumulate energy in resonance while regulating a desired amplitude. A modular and compact actuator was designed such that it can be incorporated into a range of cyclic tasks. The actuator was tested in an experiment to demonstrate the feasibility of the resonant energy accumulation under motion range limitations and realistic timing and damping conditions. In future work, we aim to use the PVSA concept in a novel hip-joint exoskeleton to increase swing leg frequency where the spring assistance torque is modulated as a function of the user's walking or running speed.

References

[1] V. R. Ham, T. G. Sugar, B. Vanderborght, K. W. Hollander, and D. Lefeber, "Compliant actuator designs: Review of actuators with passive adjustable compliance/controllable stiffness for robotic applications," *IEEE Robotics and Automation Magazine*, vol. 16, no. 3, pp. 81–94, 2009.

[2] G. Pratt and M. Williamson, "Series elastic actuators," in *IEEE/RSJ International Conference on Intelligent Robots and Systems*, vol. 1, (Pittsburgh, PA, USA), pp. 399–406, August 1995.

[3] J. Hurst, A. Rizzi, and D. Hobbelen, "Series elastic actuation: Potential and pitfalls," in *International Conference on Climbing and Walking Robots*, (Madrid, Spain), September 2004.

[4] B. Convens, D. Dong, R. Furnemont, T. Verstraten, P. Cherelle, D. Lefeber, and B. Vanderborght, "Modeling, design and test-bench validation of a semi-active propulsive ankle prosthesis with a clutched series elastic actuator," *IEEE Robotics and Automation Letters*, vol. 4, no. 2, pp. 1823–1830, 2019.

[5] E. J. Rouse, L. M. Mooney, E. C. Martinez-Villalpando, and H. M. Herr, "Clutchable series-elastic actuator: Design of a robotic knee prosthesis for minimum energy consumption," in *International Conference on Rehabilitation Robotics (ICORR)*, (Seattle, WA, USA), pp. 1–6, June 2013.

[6] D. Ragonesi, S. Agrawal, W. Sample, and T. Rahman, "Series elastic actuator control of a powered exoskeleton," in *International Conference of the IEEE Engineering in Medicine and Biology Society*, (Boston, MA, USA), pp. 3515–3518, August - September 2011.

[7] J. Hurst, J. Chestnutt, and A. Rizzi, "An actuator with physically variable stiffness for highly dynamic legged locomotion," in *IEEE International Conference on Robotics and Automation*, vol. 5, (New Orleans, LA, USA), pp. 4662–4667, April - May 2004.

[8] B. Ugurlu, C. Doppmann, M. Hamaya, P. Forni, and T. Teramae, "Control : Experiments on a Bipedal Exoskeleton," *IEEE/ASME Transactions on Mechatronics*, vol. 21, no. 1, pp. 79–87, 2016.

[9] J. Geeroms, L. Flynn, R. Jimenez-Fabian, B. Vanderborght, and D. Lefeber, "Ankle-knee prosthesis with powered ankle and energy transfer for CYBERLEGs α-prototype," in *International Conference on Rehabilitation Robotics (ICORR)*, (Seattle, WA, USA), pp. 1–6, June 2013.

[10] S. Wolf, O. Eiberger, and G. Hirzinger, "The DLR FSJ: Energy based design of a variable stiffness joint," in *IEEE International Conference on Robotics and Automation*, (Shanghai, China), pp. 5082–5089, May 2011.

[11] P. M. Wensing, A. Wang, S. Seok, D. Otten, J. Lang, and S. Kim, "Proprioceptive actuator design in the MIT cheetah: Impact mitigation and high-bandwidth physical interaction for dynamic legged robots," *IEEE Transactions on Robotics*, vol. 33, no. 3, pp. 509–522, 2017.

[12] D. F. B. Haeufle, M. D. Taylor, S. Schmitt, and H. Geyer, "A clutched parallel elastic actuator concept: Towards energy efficient powered legs in prosthetics and robotics," in *IEEE RAS EMBS International Conference on Biomedical Robotics and Biomechatronics (BioRob)*, (Rome, Italy), pp. 1614–1619, June 2012.

[13] M. Grimmer, M. Eslamy, S. Gliech, and A. Seyfarth, "A comparison of parallel- and series elastic elements in an actuator for mimicking human ankle joint in walking and running," in *IEEE International Conference on Robotics and Automation*, (Saint Paul, MN, USA), pp. 2463–2470, May 2012.

[14] B. Na and K. Kong, "Control Power Reduction and Frequency Bandwidth Enlargement of Robotic Legs by Nonlinear Resonance," *IEEE/ASME Transactions on Mechatronics*, vol. 20, no. 5, pp. 2340–2349, 2015.

[15] M. Plooij, M. Wisse, and H. Vallery, "Reducing the energy consumption of robots using the bidirectional clutched parallel elastic actuator," *IEEE Transactions on Robotics*, vol. 32, no. 6, pp. 1512–1523, 2016.

[16] S. H. Collins, M. Bruce Wiggin, and G. S. Sawicki, "Reducing the energy cost of human walking using an unpowered exoskeleton," *Nature*, vol. 522, no. 7555, pp. 212–215, 2015.

[17] R. Nasiri, A. Ahmadi, and M. N. Ahmadabadi, "Reducing the energy cost of human running using an unpowered exoskeleton," *IEEE Transactions on Neural Systems and Rehabilitation Engineering*, vol. 26, no. 10, pp. 2026–2032, 2018.

[18] T. Zhou, C. Xiong, J. Zhang, D. Hu, W. Chen, and X. Huang, "Reducing the metabolic energy of walking and running using an unpowered hip exoskeleton," *Journal of NeuroEngineering and Rehabilitation*, vol. 18, no. 1, pp. 1–15, 2021.

[19] A. Sutrisno and D. J. Braun, "Enhancing Mobility with Quasi-Passive Variable Stiffness Exoskeletons," *IEEE Transactions on Neural Systems and Rehabilitation Engineering*, vol. 27, no. 3, pp. 487–496, 2019.

[20] V. Chalvet and D. J. Braun, "Criterion for the Design of Low-Power Variable Stiffness Mechanisms," *IEEE Transactions on Robotics*, vol. 33, no. 4, pp. 1002–1010, 2017.

[21] C. English and D. Russell, "Mechanics and stiffness limitations of a variable stiffness actuator for use in prosthetic limbs," *Mechanism and machine theory*, vol. 34, no. 1, pp. 7–25, 1999.

[22] C. English and D. Russell, "Implementation of variable joint stiffness through antagonistic actuation using rolamite springs," *Mechanism and Machine Theory*, vol. 34, no. 1, pp. 27 – 40, 1999.

[23] T. Sugar and K. Hollander, "Adjustable stiffness Jack-Spring actuator," U.S. Patent No. US 8322695 B2, 2012.

[24] H. F. Lau, A. Sutrisno, T. H. Chong, and D. J. Braun, "Stiffness modulator: A novel actuator for human augmentation," in *IEEE International Conference on Robotics and Automation (ICRA)*, (Brisbane, QLD, Australia), pp. 7742–7748, May 2018.

[25] D. J. Braun, V. Chalvet, and A. Dahiya, "Positive-Negative Stiffness Actuators," *IEEE Transactions on Robotics*, vol. 35, no. 1, pp. 162–173, 2019.

[26] D. J. Braun, "Optimal Parametric Feedback Excitation of Nonlinear Oscillators," *Physical Review Letters*, vol. 116, no. 4, pp. 1–5, 2016.

[27] A. Jafari, N. G. Tsagarakis, B. Vanderborght, and D. G. Caldwell, "A novel actuator with adjustable stiffness (AwAS)," in *IEEE/RSJ International Conference on Intelligent Robots and Systems*, (Taipei, Taiwan), pp. 4201–4206, October 2010.

[28] A. Jafari, N. G. Tsagarakis, I. Sardellitti, and D. G. Caldwell, "A new actuator with adjustable stiffness based on a variable ratio lever mechanism," *IEEE/ASME Transactions on Mechatronics*, vol. 19, no. 1, pp. 55–63, 2014.

[29] B.-S. Kim and J.-B. Song, "Hybrid dual actuator unit: A design of a variable stiffness actuator based on an adjustable moment arm mechanism," in *IEEE International Conference on Robotics and Automation*, (Anchorage, AK, USA), pp. 1655–1660, May 2010.

[30] S. Groothuis, G. Rusticelli, A. Zucchelli, S. Stramigioli, and R. Carloni, "The vsaUT-II: A novel rotational variable stiffness actuator," in *IEEE International Conference on Robotics and Automation*, (Saint Paul, MN, USA), pp. 3355–3360, May 2012.

[31] D. J. Braun, V. Chalvet, C. T. Hao, S. S. Apte, and N. Hogan, "Variable Stiffness Spring Actuators for Low Energy Cost Human Augmentation," *IEEE Transactions on Robotics*, pp. 1–16, 2016.

[32] B. Vanderborght, R. V. Ham, D. Lefeber, T. G. Sugar, and K. W. Hollander, "Comparison of mechanical design and energy consumption of adaptable, passive-compliant actuators," *The International Journal of Robotics Research*, vol. 28, no. 1, pp. 90–103, 2009.

[33] R. G. Budynas, J. K. Nisbett, and J. E. Shigley, *Shigley's mechanical engineering design*. McGraw-Hill Education, 2015.

[34] J. M. Muñoz-Guijosa, D. Fernández Caballero, V. Rodríguez De La Cruz, J. L. Muñoz Sanz, and J. Echávarri, "Generalized spiral torsion spring model," *Mechanism and Machine Theory*, vol. 51, pp. 110–130, 2012.

[35] Y. Li, Z. Li, B. Penzlin, Z. Tang, Y. Liu, X. Guan, L. Ji, and S. Leonhardt, "Design of the clutched variable parallel elastic actuator (CVPEA) for lower limb exoskeletons," in *International Conference of the IEEE Engineering in Medicine and Biology Society (EMBC)*, (Berlin, Germany), pp. 4436–4439, July 2019.

[36] T. Reichert, T. Nussbaumer, and J. Kolar, "Torque scaling laws for interior and exterior rotor permanent magnet machines," in *IEEE International Magnetics Conference*, vol. 3, (Sacramento, CA, USA), pp. 4–7, May 2009.